Local-spin-density functional for multideterminant density functional theory

Simone Paziani,[1] Saverio Moroni,[2] Paola Gori-Giorgi,[3] and Giovanni B. Bachelet[1]
[1]*INFM Center for Statistical Mechanics and Complexity and Dipartimento di Fisica, Università di Roma "La Sapienza," Piazzale Aldo Moro 2, I-00185 Roma, Italy*
[2]*INFM DEMOCRITOS National Simulation Center, via Beirut 2–4, I–34014 Trieste, Italy*
[3]*Laboratoire de Chimie Théorique, CNRS UMR7616, Université Pierre et Marie Curie, 4 Place Jussieu, F-75252 Paris, France*
(Received 16 January 2006; published 14 April 2006)

Based on exact limits and quantum Monte Carlo simulations, we obtain, at any density and spin polarization, an accurate estimate for the energy of a modified homogeneous electron gas where electrons repel each other only with a long-range Coulombic tail. This allows us to construct an analytic local-spin-density exchange-correlation functional appropriate to new, multideterminantal versions of the density functional theory, where quantum chemistry and approximate exchange-correlation functionals are combined to optimally describe both long- and short-range electron correlations.

DOI: 10.1103/PhysRevB.73.155111 PACS number(s): 71.15.Mb, 71.10.Ca, 05.30.Fk, 02.70.Ss

I. INTRODUCTION

Density functional theory[1–3] (DFT) is by now the most popular method for electronic structure calculations in condensed matter physics and quantum chemistry, because of its unique combination of low computational cost and high accuracy for many molecules and solids. There are, however, exceptions to such an accuracy. Even the best approximations of its key ingredient, the exchange-correlation (XC) energy functional, cannot describe strong electron correlations, such as those of the cuprates, and cannot exactly cancel the so-called self-interaction, a property which the exact functional should satisfy. On top of that, they fail to recover long-range van der Waals interactions,[4] are not completely safe for the description of the hydrogen bond,[5] and have intrinsic problems with situations of near degeneracy (when two sets of Kohn-Sham orbitals have very close energies);[6–8] more generally, the "chemical accuracy" has not yet been reached. To overcome the latter group of problems, there has been a growing interest in "mixed schemes" which combine the DFT with other approximate methods by splitting the Coulombic electron-electron interaction $1/r=v_{ee}(r)$ into a short-range (SR) and a long-range (LR) part (see, e.g., Refs. 6–18). The idea is to use different approximations for the LR and the SR contributions to the exchange and/or correlation energy density functionals of the Kohn-Sham (KS) scheme. It descends from the observation that LR correlations, poorly described by local or semi-local density functionals, can be accurately dealt with by other techniques, like the random-phase approximation (RPA) or standard wave function methods of quantum chemistry. Conversely, correlation effects due to the SR part of the electron-electron interaction are in general well described by local or semilocal functionals.[19,20] The error function and its complement

$$\frac{1}{r}=v_{ee}(r)=v_{\mathrm{SR}}^{\mu}(r)+v_{\mathrm{LR}}^{\mu}(r)=\frac{\mathrm{erfc}(\mu r)}{r}+\frac{\mathrm{erf}(\mu r)}{r}, \quad (1)$$

where μ controls the range of the decomposition, are often used[6–8,10,11,13,15–17] to split the Coulomb interaction into a SR and a LR part, since they yield analytic matrix elements for both Gaussians and plane waves, i.e., the most common basis functions in quantum chemistry and solid state physics. Correspondingly, the universal functional of the electron density n, as defined in the constrained-search formalism[21]

$$F[n]=\min_{\Psi\to n}\langle\Psi|T+V_{ee}|\Psi\rangle \quad (2)$$

can be divided into a short-range and a complementary long-range part $F[n]=F_{\mathrm{SR}}^{\mu}[n]+\bar{F}_{\mathrm{LR}}^{\mu}[n]$

$$F_{\mathrm{SR}}^{\mu}[n]=\min_{\tilde{\Psi}^{\mu}\to n}\langle\tilde{\Psi}^{\mu}|T+V_{\mathrm{SR}}^{\mu}|\tilde{\Psi}^{\mu}\rangle,$$

$$\bar{F}_{\mathrm{LR}}^{\mu}[n]=F[n]-F_{\mathrm{SR}}^{\mu}[n] \quad (3)$$

or, alternatively, into a long-range and a complementary short-range part $F[n]=F_{\mathrm{LR}}^{\mu}[n]+\bar{F}_{\mathrm{SR}}^{\mu}[n]$

$$F_{\mathrm{LR}}^{\mu}[n]=\min_{\Psi^{\mu}\to n}\langle\Psi^{\mu}|T+V_{\mathrm{LR}}^{\mu}|\Psi^{\mu}\rangle,$$

$$\bar{F}_{\mathrm{SR}}^{\mu}[n]=F[n]-F_{\mathrm{LR}}^{\mu}[n]. \quad (4)$$

The two decompositions lead to different strategies and XC energy functionals, whose merits and drawbacks are discussed in Ref. 22. In any event, for actual electronic-structure calculations to be performed, these functionals ultimately need approximations, in analogy with the standard DFT. Regardless of the strategy adopted, the potential superiority of "mixed schemes" comes into play precisely at this stage: compared to the standard version, a DFT which only deals with the SR part of the electron-electron interaction should be much more accurately approximated, as mentioned, by local-density XC energy functionals.[15,19,20] While both decompositions [Eqs. (3) and (4)] are aimed at the exploitation of the DFT scheme for the SR part of the interaction only, the corresponding approximate functionals require an accurate description of the homogeneous electron gas (HEG) either with SR [Eq. (3)] or LR interaction [Eq. (4)].

Up to now, the HEG exchange-correlation energies as a function of the cutoff parameter μ and of the electron density are available for the SR case from quantum Monte Carlo

(QMC) simulations,[23] and for the LR case from coupled-cluster (CC) calculations.[7,24] A parametrization of the CC data for the XC energy of the HEG with long-range-only interaction has been used in Refs. 8 and 16 with very promising results for closed-shell systems. Generalized-gradient-corrected density functionals have also been designed and tested within this framework,[13,17] but all existing functionals are limited to the spin-unpolarized case.

The purpose of this paper is to provide, based on novel exact limits and quantum Monte Carlo simulations, an accurate representation for the energy of the LR-only interacting HEG not only as a function of the cutoff parameter μ and of the total electron density, but also as a function of the spin polarization [i.e., as a function of the spin densities $n_\uparrow$ and $n_\downarrow$ separately]. Since von Barth and Hedin[25] showed, in 1972, that the task of finding good approximations to exchange-correlation density functionals is greatly simplified if the functional is expressed in terms of the spin densities, and that this is the simplest way to satisfy the requirement (Hund's rule) that a state with larger spin tends to be energetically favored, the importance of including such a spin dependence in approximate functionals was confirmed by countless calculations for molecules and solids.[26,27] In this context the decomposition of Eq. (4), based on the constrained-search formalism,[21] is generalized to spin-DFT as follows:[27]

$$F^\mu_{\rm LR}[n_\uparrow,n_\downarrow] = \min_{\Psi^\mu \to n_\uparrow,n_\downarrow} \langle \Psi^\mu | T + V^\mu_{\rm LR} | \Psi^\mu \rangle,$$

$$\bar{F}^\mu_{\rm SR}[n_\uparrow,n_\downarrow] = F[n_\uparrow,n_\downarrow] - F^\mu_{\rm LR}[n_\uparrow,n_\downarrow]. \tag{5}$$

The spin-polarized LR-only gas, for which no previous results are to our knowledge available, is appropriate, via Eq. (5), to a very promising "multideterminantal" version of the spin-DFT. The final outcome of this work is thus a local-spin-density approximation of the corresponding XC functional, given in analytic form, by which electronic structure calculations of this new type will be possible for unpolarized systems[28] and, more important, for spin-polarized systems, for which no such functional is presently available. Such a functional also represents the key ingredient for extending gradient-corrected SR density functionals[13,17] to spin-DFT.

The paper is organized as follows. In Sec. II we define the Hamiltonian of the HEG with LR-only interaction and we derive some exact limits of the corresponding correlation energy, which is then computed (for values of the relevant parameters not accessible to analytic methods) with QMC in Sec. III. The results of Secs. II and III are then used in Sec. IV to construct an analytic parametrization of the LR correlation energy. Section V recalls, calculates and provides in analytic form an alternative definition of the LR correlation energy which involves the use of pair-correlation functions (also obtained from our QMC simulations) and may be of interest within optimized-effective-potential schemes.[29] Hartree atomic units are used throughout this work.

II. DEFINITIONS, AND EXACT LIMITS

After decomposing the standard (Coulomb interaction) spin-DFT functional according to Eq. (5), the resulting SR functional $\bar{F}^\mu_{\rm SR}[n_\uparrow,n_\downarrow]$ can be further decomposed, as usually, into a Hartree and an XC term

$$\bar{E}^\mu_H[n] = E^\mu_H[n] = \frac{1}{2}\int d\mathbf{r}\int d\mathbf{r}'\, n(\mathbf{r})n(\mathbf{r}')v^\mu_{\rm SR}(|\mathbf{r}-\mathbf{r}'|), \tag{6}$$

$$\bar{E}^\mu_{\rm xc}[n_\uparrow,n_\downarrow] = \bar{F}^\mu_{\rm SR}[n_\uparrow,n_\downarrow] - \bar{E}^\mu_H[n]. \tag{7}$$

The local-spin-density (LSD) approximation amounts to replacing the exact, unknown functional of Eq. (7) with

$$\begin{aligned}\bar{E}^\mu_{\rm xc,LSD}[n_\uparrow,n_\downarrow] &= \int d\mathbf{r} n(\mathbf{r})[\epsilon_{\rm xc}(n_\uparrow(\mathbf{r}),n_\downarrow(\mathbf{r})) \\ &\quad - \epsilon^{\rm LR}_{\rm xc}(n_\uparrow(\mathbf{r}),n_\downarrow(\mathbf{r}),\mu)] = \int d\mathbf{r} n(\mathbf{r}) \\ &\quad \times [\epsilon_{\rm xc}(r_s(\mathbf{r}),\zeta(\mathbf{r})) - \epsilon^{\rm LR}_{\rm xc}(r_s(\mathbf{r}),\zeta(\mathbf{r}),\mu)],\end{aligned} \tag{8}$$

where $\epsilon_{\rm xc}(n_\uparrow,n_\downarrow)$ is the exchange-correlation energy per particle of the standard jellium model[30–33] with uniform spin densities $n_\uparrow,n_\downarrow$, and $\epsilon^{\rm LR}_{\rm xc}(n_\uparrow,n_\downarrow,\mu)$ is the corresponding quantity for a jellium model with LR-only interaction $v^\mu_{\rm LR}(r)$, which forms the object of this paper. In the third line of Eq. (8) we express the same quantity in terms of the electronic density $n=n_\uparrow+n_\downarrow=(4\pi r_s^3/3)^{-1}$ and spin polarization $\zeta=(n_\uparrow-n_\downarrow)/n$, thus introducing the notation used in what follows. To obtain $\epsilon^{\rm LR}_{\rm xc}(r_s,\zeta,\mu)$ we consider a uniform system with LR-only interaction

$$H^\mu_{\rm LR} = -\frac{1}{2}\sum_{i=1}^N \nabla^2_{\mathbf{r}_i} + V^\mu_{\rm LR} + V^\mu_{eb} + V^\mu_{bb}, \tag{9}$$

where $V^\mu_{\rm LR}$ is the modified electron-electron interaction

$$V^\mu_{\rm LR} = \frac{1}{2}\sum_{i\neq j=1}^N \frac{\mathrm{erf}(\mu|\mathbf{r}_i-\mathbf{r}_j|)}{|\mathbf{r}_i-\mathbf{r}_j|}, \tag{10}$$

V^μ_{eb} is the interaction between the electrons and a rigid, positive, uniform background of density n

$$V^\mu_{eb} = -n\sum_{i=1}^N \int d\mathbf{x}\frac{\mathrm{erf}(\mu|\mathbf{r}_i-\mathbf{x}|)}{|\mathbf{r}_i-\mathbf{x}|}, \tag{11}$$

and V^μ_{bb} is the corresponding background-background interaction

$$V^\mu_{bb} = \frac{n^2}{2}\int d\mathbf{x}\int d\mathbf{x}'\frac{\mathrm{erf}(\mu|\mathbf{x}-\mathbf{x}'|)}{|\mathbf{x}-\mathbf{x}'|}. \tag{12}$$

Our Hamiltonian $H^\mu_{\rm LR}$, and thus its ground-state energy per electron $\epsilon^{\rm LR}$, depends on the density parameter r_s, on the spin-polarization ζ, and on the cutoff parameter μ. When $\mu\to\infty$, we recover the standard jellium model; in the opposite limit $\mu\to 0$, we recover the noninteracting electron gas. In this section we derive the asymptotic behavior for $\mu\to 0$ and $\mu\to\infty$ of the correlation energy per electron, defined as

$$\epsilon_c^{\mathrm{LR}}(r_s,\zeta,\mu)=\epsilon^{\mathrm{LR}}(r_s,\zeta,\mu)-t_s(r_s,\zeta)-\epsilon_x^{\mathrm{LR}}(r_s,\zeta,\mu), \quad (13)$$

where $t_s(r_s,\zeta)=3k_F^2\phi_5(\zeta)/10$ is the usual kinetic energy of the noninteracting electron gas, with $k_F=(\alpha r_s)^{-1}$, $\alpha=(4/9\pi)^{1/3}$, and

$$\phi_n(\zeta)=\frac{1}{2}[(1+\zeta)^{n/3}+(1-\zeta)^{n/3}]; \quad (14)$$

the exchange energy is given by[7]

$$\epsilon_x^{\mathrm{LR}}(r_s,\zeta,\mu)=\frac{1}{2}(1+\zeta)^{4/3}f_x(r_s,\mu(1+\zeta)^{-1/3})+\frac{1}{2}(1-\zeta)^{4/3}f_x(r_s,\mu(1-\zeta)^{-1/3}), \quad (15)$$

$$f_x(r_s,\mu)=-\frac{\mu}{\pi}\left[(2y-4y^3)e^{-1/4y^2}-3y+4y^3+\sqrt{\pi}\,\mathrm{erf}\left(\frac{1}{2y}\right)\right], \quad y=\frac{\mu\alpha r_s}{2}, \quad (16)$$

and has the asymptotic behaviors

$$\epsilon_x^{\mathrm{LR}}(r_s,\zeta,\mu)\Big|_{\mu\to 0}=-\frac{\mu}{\sqrt{\pi}}+\frac{3\alpha r_s\mu^2}{2\pi}\phi_2(\zeta)+O(\mu^3), \quad (17)$$

$$\epsilon_x^{\mathrm{LR}}(r_s,\zeta,\mu)\Big|_{\mu\to\infty}=-\frac{3k_F}{4\pi}\phi_4(\zeta)+\frac{3(1+\zeta^2)}{16r_s^3\mu^2}+O(\mu^{-4}). \quad (18)$$

A. Approaching the noninteracting gas

When $\mu\to 0$ and/or $r_s\to 0$, we are approaching the limit of the noninteracting Fermi gas. Toulouse *et al.*[15] have studied the $\mu\to 0$ limit of the long-range exchange and correlation energy functionals for confined systems (atoms, molecules) using standard perturbation theory. Their results cannot be applied to the case of an extended system like the uniform electron gas, because the integrals of their Eqs. (17) and (20) would diverge. Instead, the $\mu\to 0$ limit (as well as the $r_s\to 0$ limit) of the uniform electron gas can be studied with RPA,[25,34] which becomes exact both for long-range correlations ($\mu\to 0$: in this limit the long-range Coulombic tail shows up only beyond larger and larger interelectronic distance $r\sim 1/\mu$) and in the high-density limit ($r_s\to 0$). We generalize to the LR-only interaction $\mathrm{erf}(\mu r)/r$ the standard RPA expression for the correlation energy (see the Appendix for details), and find that, for small $\mu\sqrt{r_s}$ (i.e., small-μ and/or $r_s\to 0$ limit), the correlation energy ϵ_c^{LR} scales as

$$\epsilon_c^{\mathrm{LR}}(r_s,\zeta,\mu)\big|_{\mu,r_s\to 0}=[\phi_2(\zeta)]^3Q(x), \quad x=\frac{\mu\sqrt{r_s}}{\phi_2(\zeta)}, \quad (19)$$

where $\phi_2(\zeta)$ is given by Eq. (14), and the function $Q(x)$ has the following asymptotic behaviors:

$$Q(x\to 0)=-\frac{3\alpha}{2\pi}x^2+O(x^3), \quad (20)$$

$$Q(x\to\infty)=\frac{2\ln(2)-2}{\pi^2}\ln(x)+\mathrm{const}. \quad (21)$$

The scaling of Eq. (19) for the long-range correlation energy was also expected from the fact that the long-range part of the pair-correlation function of the standard jellium model has a similar scaling.[35–37] Notice also that, in the small-μ expansion of ϵ_c^{LR} [Eqs. (19) and (20)], the term proportional to μ^2 exactly cancels with the corresponding term in the exchange energy ϵ_x^{LR} [Eq. (17)], so that the XC energy (exchange *plus* correlation) has no μ^2 term; in a confined system, on the other hand, the μ^2 terms are separately zero for exchange and correlation.[15] We found that the function $Q(x)$ (see the Appendix) is accurately approximated by

$$Q(x)=\frac{2\ln(2)-2}{\pi^2}\ln\left(\frac{1+ax+bx^2+cx^3}{1+ax+dx^2}\right), \quad (22)$$

with $a=5.84605$, $c=3.91744$, $d=3.44851$, and $b=d-3\pi\alpha/[4\ln(2)-4]$.

A final remark on the scaling of Eq. (19) is that, although it exactly holds only in the small-x regime, even in the large-x regime of Eq. (21) (obtained e.g. with small r_s but very large μ), it represents an excellent approximation, because in this regime the ζ dependence of $\epsilon_c^{\mathrm{LR}}/Q$ is described by a function [Eq. (32) of Ref. 38] which is very similar to $[\phi_2(\zeta)]^3$, and exactly equals it for $\zeta=0$ and $\zeta=1$. All the densities corresponding to $r_s\gtrsim 0.1$ are not affected by this small difference in the ζ dependence of Eq. (19), as discussed in the Appendix.

B. Approaching the Coulombic gas

The large-μ behavior of the long-range correlation functional appropriate to the decomposition of Eq. (5), obtained in Refs. 15 and 39, is straightforwardly extended to the uniform electron gas. For $\zeta\neq 1$ we have[39]

$$\epsilon_c^{\mathrm{LR}}(r_s,\zeta,\mu)\big|_{\mu\to\infty}=\epsilon_c(r_s,\zeta)-\frac{3g_c(0,r_s,\zeta)}{8r_s^3\mu^2}-\frac{g(0,r_s,\zeta)}{\sqrt{2\pi}r_s^3\mu^3}+O(\mu^{-4}), \quad (23)$$

where $\epsilon_c(r_s,\zeta)$ is the correlation energy of the standard electron gas with Coulomb interaction, $g(0,r_s,\zeta)$ its on-top pair-distribution function,[36,37,40] and $g_c(0,r_s,\zeta)=g(0,r_s,\zeta)-\frac{1}{2}(1-\zeta^2)$. For the fully polarized gas ($\zeta=1$) the terms proportional to μ^{-2} and μ^{-3} in the large-μ expansion of ϵ_c^{LR} vanish, and the next leading terms are[39]

$$\epsilon_c^{\mathrm{LR}}(r_s,\zeta=1,\mu)\big|_{\mu\to\infty}=\epsilon_c(r_s,\zeta=1)-\frac{9g''_c(0,r_s,\zeta=1)}{64r_s^3\mu^4}-\frac{9g''(0,r_s,\zeta=1)}{40\sqrt{2\pi}r_s^3\mu^5}+O(\mu^{-6}), \quad (24)$$

where $g''(0,r_s,\zeta=1)$ is the second derivative at $r=0$ of the

pair-distribution function[36,37,40] of the fully polarized gas, and $g_c''(0,r_s,\zeta=1)=g''(0,r_s,\zeta=1)-2^{5/3}k_F^2/5$.

III. DIFFUSION MONTE CARLO

The details of the simulations are similar to our previous calculation of a local density functional for a short-range potential.[23] Here we give a technical summary focusing on the main differences, which concern the size extrapolation and the treatment of the long-range tails of the interaction and of the pair pseudopotential in the trial wave function. For the reader not keen on technicalities, it is enough to say that we provide a very tight upper bound to the exact ground-state energy, choosing a level of approximation which closely matches the Ceperley-Alder[30] (CA) result for $\mu\to\infty$.

The ground-state energy of the Hamiltonian of Eq. (9) is computed with the diffusion Monte Carlo (DMC) method in the fixed-node (FN) approximation,[41] using a standard Jastrow-Slater trial function with plane-wave orbitals and RPA pseudopotentials.[42] Several values of the density ($r_s=1,2,5$, and 10), of the cutoff parameter ($\mu r_s=0.5,1,2$, and 4) and of the spin polarization ($\zeta=0$ and 1) are considered. The results are fitted (see Sec. IV) to a convenient analytical expression for the correlation energy $\epsilon_c(r_s,\mu,\zeta)$, which also embodies the exact limits of Sec. II and is further constrained to recover the CA result for the Coulomb potential.

This constraint sets the target precision of our simulations, since there is no point in pushing the accuracy much beyond the statistical uncertainty of the CA results. Correspondingly, we make sure that the biases due to a finite time step and a finite number of walkers are much smaller than the statistical uncertainties of the CA results. Furthermore, as discussed in Ref. 23, a smoother match to the CA results of the FN energy in the $\mu\to\infty$ limit is expected using the nodal structure given by Slater determinants of plane waves, instead of the more accurate[43] (and computationally more demanding) backflow nodes.

We simulate N particles in a cubic box with "twist-averaged boundary conditions"[44] (TABC), which have been shown to eliminate most of the finite-size effect due to the shell structure of the plane-wave determinants. For each system considered, simulations are performed for 35 points in the irreducible wedge of the first Brillouin zone (BZ) of the simulation box, corresponding to a 1000-point mesh in the whole BZ.

Both the interparticle potential and the RPA pair pseudopotential are computed using an optimized breakup[45] into a long-range part, to be treated in reciprocal space, and a short-range part, to be treated in real space. The short-range part is expanded in locally piecewise quintic Hermite interpolants over 20 knots, and the k-space summation includes 20 shells of reciprocal lattice vectors. This choice of parameters ensures that, for the Coulomb interaction, the potential energy calculated for a simulation box containing 64 particles on a simple cubic lattice reproduces the exact Madelung constant to less than 1 part in 10^7.

All DMC simulations have been done with $N=54$ for both the paramagnetic and the spin-polarized fluids (there is no need of choosing closed-shell determinants with TABC).

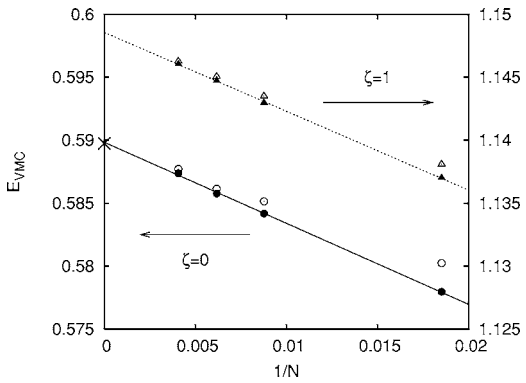

FIG. 1. The size dependence of the VMC energy for the Coulomb potential at $r_s=1$. Empty symbols: VMC energy E_N; filled symbols: $E_N+T_\infty-T_N$. The curves show the best-fit $1/N$ dependence of the latter, according to Eq. (25): circles and solid line refer to $\zeta=0$ (left scale), triangles and dashed line to $\zeta=1$ (right scale). The cross is the $\zeta=0$ result obtained in the thermodynamic limit by Ref. 43, which appears fully consistent with the present calculation. The statistical errors on the data points are much smaller than the symbol sizes. The χ^2 is 11.8 for $\zeta=0$, and 0.4 for $\zeta=1$ (much poorer values would be obtained by just fitting E_{VMC}, i.e., without including the kinetic-energy size correction).

Following a common practice,[30,43] the residual size effect has been estimated assuming that it is the same for DMC and Variational Monte Carlo (VMC),[41] which is somewhat less accurate but much cheaper. Systems with up to 246 particles were simulated with the VMC algorithm, and the size dependence of the computed energies E_N was modeled as

$$E_\infty = E_N + T_\infty - T_N + \beta/N, \tag{25}$$

where T_∞ and T_N are the kinetic energy in the thermodynamic limit and in the N-particle system (with TABC), respectively, and E_∞ and β are fitting parameters. The χ^2 value, less than 2 on average, is at worst about 10 for $r_s=1$ and $\mu=4$, at $\zeta=0$. Figure 1 shows the size extrapolation procedure for the Coulomb potential at $r_s=1$. Since the dependence on spin polarization of the optimal value of β is very weak (see Fig. 1), a systematic study of the finite-size effect was carried out only for $\zeta=0$: for given μ and r_s, the same value of β, determined from the VMC energies of the paramagnetic fluid at several system sizes, was then used to estimate the finite-size correction to the DMC energy for both $\zeta=0$ and $\zeta=1$. For the unpolarized gas, we found that the discrepancies on the correlation energy with the coupled-cluster data of Refs. 7 and 24 are of the order of 5–8%.

IV. ANALYTIC REPRESENTATION OF THE CORRELATION ENERGY

We construct an analytical representation of the correlation energy as

$$\epsilon_c^{\mathrm{LR}}(r_s,\zeta,\mu)=\frac{[\phi_2(\zeta)]^3 Q\left(\frac{\mu\sqrt{r_s}}{\phi_2(\zeta)}\right)+a_1\mu^3+a_2\mu^4+a_3\mu^5+a_4\mu^6+a_5\mu^8}{(1+b_0^2\mu^2)^4}, \tag{26}$$

where the function Q is given by Eq. (22), the parameters $a_i(r_s,\zeta)$ ensure the correct large-μ behavior of Eqs. (23), (24), and $b_0(r_s)$ is fixed by a best fit to our DMC data. Some more free parameters which are adjusted to fit the DMC data are also contained in the coefficients $a_i(r_s,\zeta)$, whose definition requires a detailed explanation. For the limits of Eqs. (23), (24) we use, for any spin polarization ζ, the approximation

$$\begin{aligned}\epsilon_c^{\mathrm{LR}}(r_s,\zeta,\mu)\big|_{\mu\to\infty}\approx{}&\epsilon_c(r_s,\zeta)-\frac{3(1-\zeta^2)g_c(0,r_s,\zeta=0)}{8r_s^3\mu^2}\\&-(1-\zeta^2)\frac{g(0,r_s,\zeta=0)}{\sqrt{2\pi}r_s^3\mu^3}-\frac{9c_4(r_s,\zeta)}{64r_s^3\mu^4}\\&-\frac{9c_5(r_s,\zeta)}{40\sqrt{2\pi}r_s^3\mu^5}+O(\mu^{-6}),\ \text{with}\end{aligned} \tag{27}$$

$$\begin{aligned}c_4(r_s,\zeta)={}&\left(\frac{1+\zeta}{2}\right)^2 g''\left(0,r_s\left(\frac{2}{1+\zeta}\right)^{1/3},\zeta=1\right)\\&+\left(\frac{1-\zeta}{2}\right)^2 g''\left(0,r_s\left(\frac{2}{1-\zeta}\right)^{1/3},\zeta=1\right)\\&+(1-\zeta^2)D_2(r_s)-\frac{\phi_8(\zeta)}{5\alpha^2 r_s^2},\ \text{and}\end{aligned} \tag{28}$$

$$\begin{aligned}c_5(r_s,\zeta)={}&\left(\frac{1+\zeta}{2}\right)^2 g''\left(0,r_s\left(\frac{2}{1+\zeta}\right)^{1/3},\zeta=1\right)\\&+\left(\frac{1-\zeta}{2}\right)^2 g''\left(0,r_s\left(\frac{2}{1-\zeta}\right)^{1/3},\zeta=1\right)\\&+(1-\zeta^2)D_3(r_s).\end{aligned} \tag{29}$$

The function ϕ_8 is defined by Eq. (14); $D_2(r_s)$ and $D_3(r_s)$ mimic the effect of the $\uparrow\downarrow$ correlation on the μ^{-4} and μ^{-5} large-μ coefficients, and are obtained by a best fit to the DMC data. For the parallel-spin $g''(0,r_s,\zeta)$ and for the on-top $g(0,r_s,\zeta)$ an exchangelike ζ dependence was assumed, starting from the values at $\zeta=1$ and $\zeta=0$, respectively. The on-top $g(0,r_s,\zeta=0)$ was taken from Ref. 40, while $g''(0,r_s,\zeta=1)$ was obtained as a best fit to our DMC data. The parameters $a_i(r_s,\zeta)$ of Eq. (26) are then equal to

$$a_1=4b_0^6C_3+b_0^8C_5,$$

$$a_2=4b_0^6C_2+b_0^8C_4+6b_0^4\epsilon_c,$$

$$a_3=b_0^8C_3,$$

$$a_4=b_0^8C_2+4b_0^6\epsilon_c,$$

$$a_5=b_0^8\epsilon_c,$$

where $\epsilon_c(r_s,\zeta)$ is the parametrization of the CA correlation energy as given by Perdew and Wang,[33] and

$$C_2=-\frac{3(1-\zeta^2)g_c(0,r_s,\zeta=0)}{8r_s^3},$$

$$C_3=-(1-\zeta^2)\frac{g(0,r_s,\zeta=0)}{\sqrt{2\pi}r_s^3},$$

$$C_4=-\frac{9c_4(r_s,\zeta)}{64r_s^3},$$

$$C_5=-\frac{9c_5(r_s,\zeta)}{40\sqrt{2\pi}r_s^3}. \tag{30}$$

The functions b_0, g'', D_2, and D_3 are finally obtained from a best fit to the DMC data and read

$$b_0(r_s)=0.784949r_s, \tag{31}$$

$$g''(0,r_s,\zeta=1)=\frac{2^{5/3}}{5\alpha^2r_s^2}\frac{1-0.02267r_s}{(1+0.4319r_s+0.04r_s^2)}, \tag{32}$$

$$D_2(r_s)=\frac{e^{-0.547r_s}}{r_s^2}(-0.388r_s+0.676r_s^2), \tag{33}$$

$$D_3(r_s)=\frac{e^{-0.31r_s}}{r_s^3}(-4.95r_s+r_s^2). \tag{34}$$

Notice that, by our construction, Eq. (32) satisfies the exact high-density limit.[46] Our data and the fitting function of Eq. (26) are shown in Fig. 2. The small discrepancy at large μ, particularly visible for $r_s=1$ and $\zeta=1$ on the scales of the figure, is due to the condition that our fitting function recovers in the Coulomb limit the Perdew-Wang parametrization[33] of the CA correlation energy, and it is consistent with our FN results being an upper bound to the data obtained[30] by CA using a nominally exact method.

V. PAIR-DISTRIBUTION FUNCTIONS AND ALTERNATIVE SEPARATION OF EXCHANGE AND CORRELATION

From our DMC runs we also extracted, in the usual way,[47] the pair-distribution functions $g^{\mathrm{LR}}(r,r_s,\zeta,\mu)$. A sample of our results is shown in Fig. 3. These functions are of interest in the framework of the approach of Refs. 7, 8, and 13–17. While a local- (or local-spin-) density approximation for

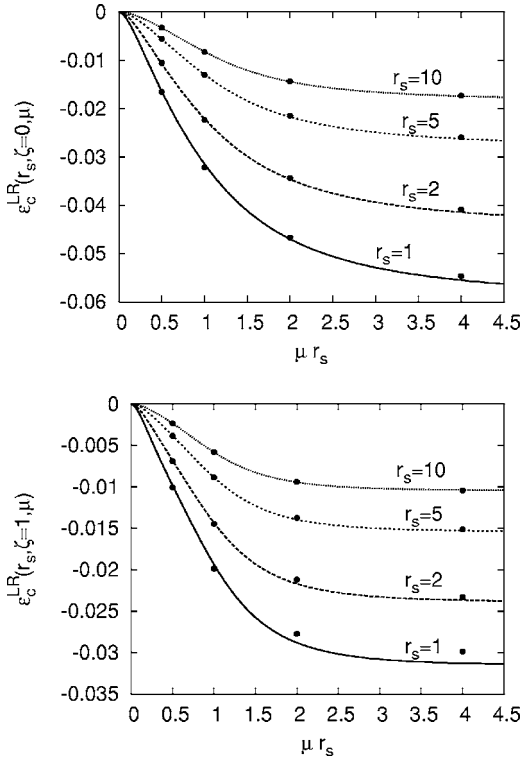

FIG. 2. Our DMC data for the correlation energy (•) of the electron gas with long-range interaction $\mathrm{erf}(\mu r)/r$ are compared with the fitting function (lines) of Eq. (26) for the unpolarized case (upper panel) and the fully polarized case (lower panel). The statistical errors on the DMC data are comparable with the symbol size.

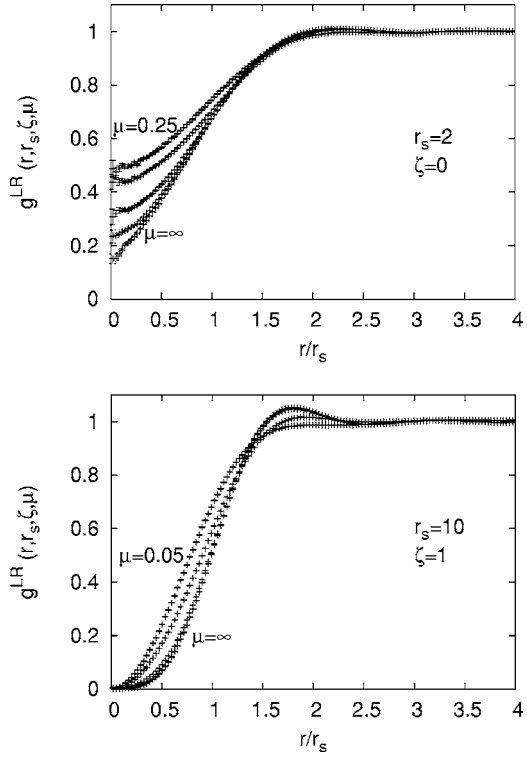

FIG. 3. A sample of our DMC pair-distribution functions. Upper panel: for $r_s=2$ and $\zeta=0$, g^{LR} is shown for $\mu=0.25, 0.5, 1, 2$, and for the Coulomb gas ($\mu=\infty$). Lower panel: for $r_s=10$ and $\zeta=1$, g^{LR} is shown for $\mu=0.05, 0.1, 0.2, 0.4$, and for the Coulomb gas ($\mu=\infty$).

both exchange and correlation has been, and to a large extent still is, the most popular approach to Kohn-Sham calculations (possibly with GGA improvements), there is a growing interest[48] in optimized-effective-potential schemes, where the exchange is treated exactly and the construction of approximations only concerns the correlation energy. The latter is naturally defined as whatever exceeds the exact-exchange energy, obtained from a single Slater determinant of Kohn-Sham orbitals. But once a multideterminantal, partially correlated wave function Ψ^μ [Eq. (5)] is introduced, as in the modified schemes we are concerned with here, an alternative, more efficient choice may be to construct approximations only for that portion of the correlation energy which is not already taken into account by Ψ^μ. In other words, one may prefer to define[29] "exchange" and "correlation" energy functionals in the following way:

$$\bar{E}^{\mu}_{x,\mathrm{md}}[n_\uparrow,n_\downarrow] = \langle\Psi^\mu|V_{ee} - V^{\mu}_{\mathrm{LR}}|\Psi^\mu\rangle - \bar{E}^{\mu}_{H}[n], \tag{35}$$

$$\bar{E}^{\mu}_{c,\mathrm{md}}[n_\uparrow,n_\downarrow] = \bar{E}^{\mu}_{\mathrm{xc}}[n_\uparrow,n_\downarrow] - \bar{E}^{\mu}_{x,\mathrm{md}}[n_\uparrow,n_\downarrow], \tag{36}$$

and then apply, e.g., the LSD approximation only to the "correlation" energy functional of Eq. (36):[29]

$$\bar{E}^{\mu}_{c,\mathrm{md}}[n_\uparrow,n_\downarrow] = \int d\mathbf{r} n(\mathbf{r}) \bar{\epsilon}_{\mathrm{c,md}}(r_s(\mathbf{r}),\zeta(\mathbf{r}),\mu). \tag{37}$$

Here

$$\bar{\epsilon}_{\mathrm{c,md}}(r_s,\zeta,\mu) = \epsilon_c(r_s,\zeta) - \epsilon_c^{\mathrm{LR}}(r_s,\zeta,\mu) + \Delta_{\mathrm{LR\text{-}SR}}(r_s,\zeta,\mu), \tag{38}$$

the mixed term $\Delta_{\mathrm{LR\text{-}SR}}(r_s,\zeta,\mu)$ is equal to

$$\Delta_{\mathrm{LR\text{-}SR}}(r_s,\zeta,\mu) = -\frac{n}{2}\int_0^\infty 4\pi r^2 dr g_c^{\mathrm{LR}}(r,r_s,\zeta,\mu)\frac{\mathrm{erfc}(\mu r)}{r}, \tag{39}$$

and g_c^{LR} is given by g^{LR} minus the pair-distribution function of the noninteracting gas. Using the results of Ref. 39 it is easy to show that, for large μ, the mixed term $\Delta_{\mathrm{LR\text{-}SR}}$ behaves as

$$\Delta_{\mathrm{LR\text{-}SR}}\Big|_{\mu\to\infty} = -\frac{3g_c(0,r_s,\zeta)}{8r_s^3\mu^2} - \frac{g(0,r_s,\zeta)(2\sqrt{2}-1)}{2\sqrt{\pi}r_s^3\mu^3} + O(\mu^{-4}) \tag{40}$$

for $\zeta\neq 1$, and as

$$\Delta_{\mathrm{LR\text{-}SR}}\Big|_{\mu\to\infty} = -\frac{9g_c''(0,r_s,\zeta=1)}{64r_s^3\mu^4} - \frac{3g''(0,r_s,\zeta=1)(3-\sqrt{2})}{20\sqrt{2\pi}r_s^3\mu^5} + O(\mu^{-6}) \tag{41}$$

for $\zeta=1$, with the same notations of Eqs. (23), (24).

In this section we present an accurate parametrization of $\Delta_{\text{LR-SR}}$. Exploiting our DMC pair-distribution functions $g^{\text{LR}}(r,r_s,\zeta,\mu)$, we solved Eq. (39) by numerical integration, and parametrized our results as

$$\Delta_{\text{LR-SR}} = \frac{\delta_2\mu^2 + \delta_3\mu^3 + \delta_4\mu^4 + \delta_5\mu^5 + \delta_6\mu^6}{(1+d_0^2\mu^2)^4}, \quad (42)$$

where the functions $\delta_i(r_s,\zeta)$ with $i=3$–6 guarantee the correct large-μ behavior of Eqs. (40), (41):

$$\delta_3 = 4d_0^6\widetilde{C}_3 + d_0^8\widetilde{C}_5, \quad (43)$$

$$\delta_4 = 4d_0^6 C_2 + d_0^8 C_4, \quad (44)$$

$$\delta_5 = d_0^8\widetilde{C}_3, \quad (45)$$

$$\delta_6 = d_0^8 C_2. \quad (46)$$

Here $C_2(r_s,\zeta)$ and $C_4(r_s,\zeta)$ are those of Eqs. (30);

$$\widetilde{C}_3 = -(1-\zeta^2)\frac{g(0,r_s,\zeta=0)(2\sqrt{2}-1)}{2\sqrt{\pi}r_s^3},$$

$$\widetilde{C}_5 = -\frac{3c_5(r_s,\zeta)(3-\sqrt{2})}{20\sqrt{2\pi}r_s^3}; \quad (47)$$

$g(0,r_s,\zeta=0)$ and $c_5(r_s,\zeta)$ are defined in Sec. IV. The remaining parameters $\delta_2(r_s)$ and $d_0(r_s,\zeta)$ are fitted to our DMC data and read

$$\delta_2(r_s) = 0.073867r_s^{3/2}, \quad (48)$$

$$d_0(r_s,\zeta) = (0.70605 + 0.12927\zeta^2)r_s. \quad (49)$$

VI. CONCLUSIONS

We have presented a comprehensive numerical and analytic study of the ground-state energy of a homogeneous electron gas with modified, long-range-only electron-electron interaction $\text{erf}(\mu r)/r$, as a function of the cutoff parameter μ, of the electronic density, and of spin polarization. The final outcome of this work is the publication of a reliable local-spin-density functional which fits the results of our quantum Monte Carlo simulations and automatically incorporates exact limits. Such a functional (Sec. IV), or its variant implying the use of an additional term also obtained in this work (Sec. V), are the key ingredient for some recently proposed "multideterminantal" versions of the density functional theory, where quantum chemistry and approximate exchange-correlation functionals are combined to optimally describe both long- and short-range electron correlations. A FORTRAN subroutine that evaluates our LSD exchange-correlation functional and the corresponding potentials is available upon request to gori@lct.jussieu.fr, or can be downloaded at http://www.lct.jussieu.fr/DFT/gori/elegas.html.

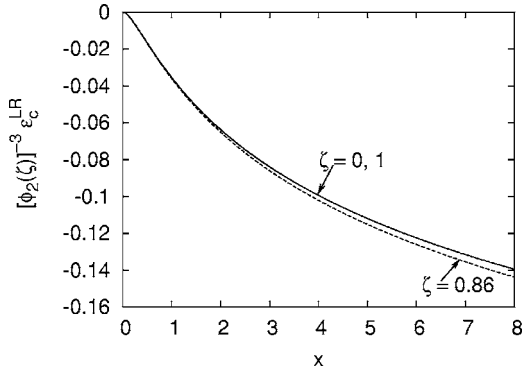

FIG. 4. The numerical evaluation of Eq. (A1), as a function of $x=\mu\sqrt{r_s}/\phi_2(\zeta)$, and multiplied by $[\phi_2(\zeta)]^{-3}$. If the scaling of Eq. (19) were exact, all the values corresponding to different ζ would lie on the solid curve. The value $\zeta=0.86$ shown in the figure corresponds to the maximum deviation from the scaling of Eq. (A1).

ACKNOWLEDGMENTS

We thank A. Savin and J. Toulouse for useful discussions, H. Stoll and J.G. Ángyán for suggesting and encouraging this work, and gratefully acknowledge financial support from the Italian Ministry of Education, University and Research (MIUR) through COFIN 2005-2006 and the allocation of computer resources from INFM Iniziativa Calcolo Parallelo.

APPENDIX: DETAILS OF EQ. (19)

We start from the RPA equations[25] for the spin-polarized electron gas, and we simply replace the Coulomb interaction $1/r$ with the long-range interaction $\text{erf}(\mu r)/r$. We then repeat the analysis done in Refs. 35 and 38 for the Coulombic gas and find that, in the $r_s\to 0$ limit, the correlation energy is given by

$$\epsilon_c^{\text{LR}}(r_s,\zeta,\mu)\big|_{r_s\to 0} = -\frac{12}{\pi}\int_0^\infty \frac{dy}{\alpha^2}y\int_0^\infty du\left\{\alpha R_\zeta(u)e^{-(y/\alpha\mu\sqrt{r_s})^2} - y^2\ln\left[1+\frac{\alpha}{y^2}R_\zeta(u)e^{-(y/\alpha\mu\sqrt{r_s})^2}\right]\right\}, \quad (A1)$$

where

$$R_\zeta(u) = \frac{1}{2}\left[z_1 R\left(\frac{u}{z_1}\right) + z_2 R\left(\frac{u}{z_2}\right)\right], \quad (A2)$$

with

$$R(u) = \frac{1}{\pi}[1 - u\arctan(u^{-1})], \quad (A3)$$

$z_1=(1+\zeta)^{1/3}$, $z_2=(1-\zeta)^{1/3}$, and $\alpha=(4/9\pi)^{1/3}$. Equation (A1) already shows that the correlation energy becomes a function of $\mu\sqrt{r_s}$ in the $r_s\to 0$ limit.

To prove the small-x behavior of Eq. (20), take a value of $\mu\sqrt{r_s}=a\ll 1$. In this case all the contribution to the integral of Eq. (A1) comes from small y, since, as soon as $y\gg a$, the integrand goes to zero exponentially fast, as a function of a, when $a\to 0$. We thus integrate over y Eq. (A1) between 0

and a value q_1 such that $a \ll q_1 \ll 1$. Since $y \ll 1$, the integral reduces to

$$-\frac{12}{\pi\alpha}\int_0^{q_1} dyye^{-(y/\alpha a)^2}\int_0^{\infty} duR_\zeta(u), \tag{A4}$$

which gives, to leading orders in a when $a \to 0$, Eqs. (19) and (20). The large x behavior of Eq. (21) follows by considering the $\mu \to \infty$ limit of Eq. (A1), which reduces to the standard Coulombic case studied in Ref. 38.

The ζ dependence of Eq. (19) is exact in the $x \to 0$ limit of Eq. (A4). For larger x, we evaluated Eq. (A1) numerically, and in Fig. 4 we report our results multiplied by $[\phi_2(\zeta)]^{-3}$, as a function of $x = \mu\sqrt{r_s}/\phi_2(\zeta)$: if the scaling of Eq. (19) were exact, all the values corresponding to different ζ would lie on the solid curve, corresponding to $\zeta = 0$ and 1. The value $\zeta = 0.86$ reported in the figure corresponds to the maximum deviation from the scaling of Eq. (19), which is thus rather small. The function $Q(x)$ of Eq. (22) has been obtained by fitting the RPA data of the solid curve. On the scale of Fig. 4 the fitting error is invisible.

To conclude the discussion, we expect that the correlation energy ϵ_c^{LR} lies on the curve of Fig. 4 when $\mu r_s \ll 1$ (high-density or really long-range-only interaction on the scale r_s). This means that at a given r_s, the "exact" ϵ_c^{LR} lies on the curve of Fig. 4 for values of μ such that $\mu\sqrt{r_s} \lesssim 1/\sqrt{r_s}$, that is, only the densities $r_s \lesssim 0.1$ would be affected by the small deviations from the scaling in ζ of Eq. (19), which appear at $x \gtrsim 3$.

[1] W. Kohn, Rev. Mod. Phys. **71**, 1253 (1999).
[2] A. E. Mattsson, Science **298**, 759 (2002).
[3] *A Primer in Density Functional Theory*, edited by C. Fiolhais, F. Nogueira, and M. Marques (Springer-Verlag, Berlin, 2003).
[4] In this paper we deal with the separation of the long-range and the short-range part of the electron-electron interaction within DFT, a strategy which can efficiently describe van der Waals interactions (Refs. 9 and 16). For other, recent, promising attempts to take into account dispersion forces within DFT see, e.g., M. Dion, H. Rydberg, E. Schröder, D. C. Langreth, and B. I. Lundqvist, Phys. Rev. Lett. **92**, 246401 (2004); J. Dobson, J. Wang, B. Dinte, K. McLennan, and H. Le, Int. J. Quantum Chem. **101**, 579 (2005); E. Johnson and A. Becke, J. Chem. Phys. **123**, 024101 (2005); A. Becke and E. Johnson, *ibid.* **122**, 154104 (2005); A. Becke and E. Johnson, *ibid.* **123**, 154101 (2005).
[5] J. Ireta, J. Neugebauer, and M. Scheffler (unpublished).
[6] H. Stoll and A. Savin, in *Density Functional Method in Physics*, edited by R. M. Dreizler and J. da Providencia (Plenum, Amsterdam, 1985).
[7] A. Savin, in *Recent Developments and Applications of Modern Density Functional Theory*, edited by J. M. Seminario (Elsevier, Amsterdam, 1996).
[8] T. Leininger, H. Stoll, H.-J. Werner, and A. Savin, Chem. Phys. Lett. **275**, 151 (1997); R. Pollet, A. Savin, T. Leininger, and H. Stoll, J. Chem. Phys. **116**, 1250 (2002).
[9] W. Kohn, Y. Meir, and D. E. Makarov, Phys. Rev. Lett. **80**, 4153 (1998).
[10] H. Ikura, T. Tsuneda, T. Yanai, and K. Hirao, J. Chem. Phys. **115**, 3540 (2001); M. Kamiya, T. Tsuneda, and K. Hirao, *ibid.* **117**, 6010 (2002); T. T. Y. Tawada, S. Yanagisawa, T. Yanai, and K. Hirao, *ibid.* **120**, 8425 (2004).
[11] J. Heyd, G. E. Scuseria, and M. Ernzerhof, J. Chem. Phys. **118**, 8207 (2003).
[12] R. Baer and D. Neuhauser, Phys. Rev. Lett. **94**, 043002 (2005).
[13] J. Toulouse, F. Colonna, and A. Savin, J. Chem. Phys. **122**, 014110 (2005).
[14] R. Pollet, F. Colonna, T. Leininger, H. Stoll, H.-J. Werner, and A. Savin, Int. J. Quantum Chem. **91**, 84 (2003).
[15] J. Toulouse, F. Colonna, and A. Savin, Phys. Rev. A **70**, 062505 (2004).
[16] J. G. Ángyán, I. C. Gerber, A. Savin, and J. Toulouse, Phys. Rev. A **72**, 012510 (2005); I. Gerber and J. G. Ángyán, Chem. Phys. Lett. **415**, 100 (2005).
[17] E. Goll, H.-J. Werner, and H. Stoll, Phys. Chem. Chem. Phys. **7**, 3917 (2005).
[18] S. Yamanaka, K. Kusakabe, K. Nakata, T. Takada, and K. Yamaguchi, physics/0508121 (unpublished).
[19] K. Burke, J. P. Perdew, and M. Ernzerhof, J. Chem. Phys. **109**, 3760 (1998).
[20] J. P. Perdew, A. Savin, and K. Burke, Phys. Rev. A **51**, 4531 (1995).
[21] M. Levy, Proc. Natl. Acad. Sci. U.S.A. **76**, 6062 (1979).
[22] J. Toulouse and A. Savin, J. Mol. Struct.: THEOCHEM (to be published).
[23] L. Zecca, P. Gori-Giorgi, S. Moroni, and G. B. Bachelet, Phys. Rev. B **70**, 205127 (2004).
[24] A. Savin and H.-J. Flad, Int. J. Quantum Chem. **56**, 327 (1995); J. Toulouse, A. Savin, and H.-J. Flad, *ibid.* **100**, 1047 (2004).
[25] U. von Barth and L. Hedin, J. Phys. C **5**, 1629 (1972).
[26] R. O. Jones and O. Gunnarsson, Rev. Mod. Phys. **61**, 689 (1989).
[27] A. Nagy, Phys. Rep. **298**, 1 (1998).
[28] QMC provides the most accurate numerical values for several physical properties of the HEG. See, e.g., G. Giuliani and G. Vignale, *Quantum Theory of the Electron Liquid* (Cambridge University Press, Cambridge, 2005); D. M. Ceperley, in *The Electron Liquid Paradigm in Condensed Matter Physics*, edited by G. F. Giuliani and G. Vignale (IOS, Amsterdam, 2004).
[29] J. Toulouse, P. Gori-Giorgi, and A. Savin, Theor. Chim. Acta **114**, 305 (2005).
[30] D. M. Ceperley and B. J. Alder, Phys. Rev. Lett. **45**, 566 (1980).
[31] S. H. Vosko, L. Wilk, and M. Nusair, Can. J. Phys. **58**, 1200 (1980).
[32] J. P. Perdew and A. Zunger, Phys. Rev. B **23**, 5048 (1981).
[33] J. P. Perdew and Y. Wang, Phys. Rev. B **45**, 13244 (1992).
[34] See, e.g., D. Pines and P. Nozières, *Theory of Quantum Liquids* (Benjamin, New York, 1966).
[35] Y. Wang and J. P. Perdew, Phys. Rev. B **44**, 13298 (1991).
[36] J. P. Perdew and Y. Wang, Phys. Rev. B **46**, 12947 (1992); **56**, 7018(E) (1997).

[37] P. Gori-Giorgi and J. P. Perdew, Phys. Rev. B **66**, 165118 (2002).
[38] Y. Wang and J. P. Perdew, Phys. Rev. B **43**, 8911 (1991).
[39] P. Gori-Giorgi and A. Savin, Phys. Rev. A **73**, 032506 (2006).
[40] P. Gori-Giorgi and J. P. Perdew, Phys. Rev. B **64**, 155102 (2001).
[41] For a recent review on fixed-node diffusion Monte Carlo and further references, see M. Foulkes, L. Mitas, R. Needs, and G. Rajagopal, Rev. Mod. Phys. **73**, 33 (2001).
[42] D. Ceperley, Phys. Rev. B **18**, 3126 (1978).
[43] Y. Kwon, D. M. Ceperley, and R. M. Martin, Phys. Rev. B **58**, 6800 (1998).
[44] C. Lin, F. H. Zong, and D. M. Ceperley, Phys. Rev. E **64**, 016702 (2001).
[45] V. Natoli and D. M. Ceperley, J. Comput. Phys. **117**, 171 (1995).
[46] V. A. Rassolov, J. A. Pople, and M. A. Ratner, Phys. Rev. B **62**, 2232 (2000).
[47] See, e.g., G. Ortiz and P. Ballone, Phys. Rev. B **50**, 1391 (1994); **56**, 9970(E) (1997).
[48] See, e.g., S. Kümmel and J. P. Perdew, Phys. Rev. B **68**, 035103 (2003); W. Yang and Q. Wu, Phys. Rev. Lett. **89**, 143002 (2002); R. J. Magyar, A. Fleszar, and E. K. U. Gross, Phys. Rev. B **69**, 045111 (2004); M. Grüning, O. V. Gritsenko, and E. J. Baerends, J. Chem. Phys. **118**, 7183 (2003). For a critical review, see also E. J. Baerends and O. V. Gritsenko, *ibid.* **123**, 062202 (2005).